

---

# How to Instruct Your Robot: Dense Language Annotations Power Robot Policy Learning

---

Bosung Kim<sup>1,2\*</sup> Ruiyi Wang<sup>1\*</sup> David Acuna<sup>2</sup> Jaehun Jung<sup>2</sup>  
Alexander Trevithick<sup>2</sup> Brandon Cui<sup>2</sup> Yejin Choi<sup>2</sup> Prithviraj Ammanabrolu<sup>1,2</sup>  
<sup>1</sup>University of California, San Diego <sup>2</sup>NVIDIA

## Abstract

Scaling robot policy learning is bottlenecked by the cost of collecting demonstrations: datasets at modern scale require thousands of skilled-operator hours on dedicated robot hardware. The language description paired with these demonstrations does not face the same bottleneck—a single short task label is cheap, but it also leaves implicit spatial relations, object interactions, embodiment state, and subgoal structure that the pixels already contain. We treat *language density* as a cheap lever for amplifying signal in a fixed demonstration corpus; whereas prior dense-language work in robotics commits to a single caption style, we instead ask which kind of dense language helps each task and learn to deliver it at deployment. We realize this as **DeMiAn (Dense Multi-aspect Annotation)** in two stages. First, an automatic VLM pipeline re-labels each segment of an existing demonstration along four complementary aspects—*physical motion*, *scene composition*, *arm pose*, and segment-level *reasoning*—each surfacing a distinct kind of structure that a one-line task label omits. Second, a small learned *instructor*, trained via supervised fine-tuning, maps the natural language task description and an initial scene snapshot to a task-appropriate annotation and runs asynchronously alongside the action policy, hiding generation latency behind the rollout. Applied to more than 1M robot manipulation and 50K EgoVerse human-egocentric videos, with no new demonstrations collected, DeMiAn delivers four findings on a VLA action policy and a video-based world-action model: (i) the learned instructor raises RoboCasa success rate by 5 percentage points over the no-annotation baseline, within 3 points of a per-task oracle; (ii) that oracle is non-trivial—no fixed aspect dominates, and peak performance requires selecting the right annotation aspect per task; (iii) the trained system extends usefully to composite tasks under subgoal-driven prompt switching, and to OOD scenes and objects; and (iv) dense annotation improves the compute-performance frontier in both mid-training and post-training, making re-annotation a practical scaling lever for robot policy learning.

## 1 Introduction

The dominant paradigm in robot learning today is scaling: more demonstrations, more environments, more diverse embodiments [35, 8, 18]. Vision-language-action (VLA) models have emerged at the center of this effort, unifying visual perception, language understanding, and action generation within a single architecture [6, 41, 5, 19, 4]. A more recent shift toward video-based world-action models (WAMs) extends this trajectory by mid-training on human-egocentric or web video before any robot data is seen, leveraging the fact that web video datasets scale far beyond robot teleoperation [11, 38, 29]. Across both directions, the bottleneck is the same: datasets at modern scale require thousands of skilled-operator hours on dedicated robot hardware before any policy training begins, and even

---

\*Equal contribution.

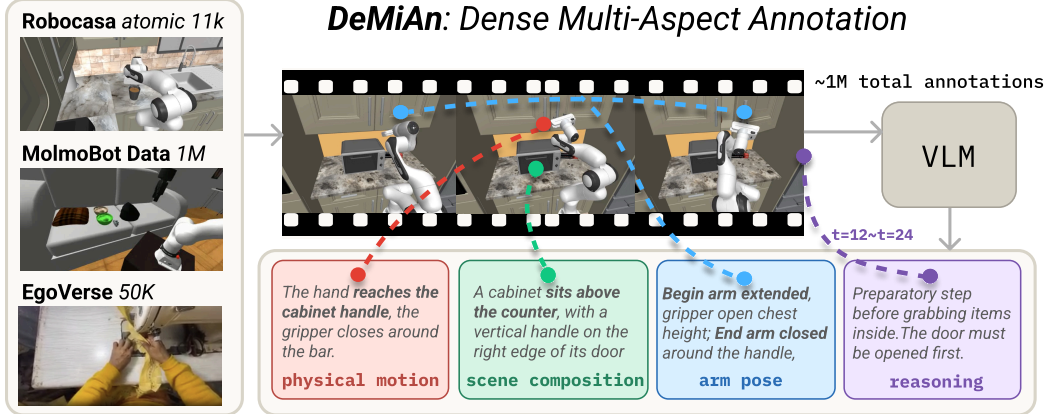


Figure 1: **Overview of DeMiAn.** We re-annotate existing robot and human demonstrations along four aspects: *physical motion*, *scene composition*, *arm pose*, and *reasoning*. We apply DeMiAn to 11K RoboCasa 365 clips, a 1M-scale MolmoBot dataset, and 50K EgoVerse human-egocentric clips.

human-egocentric datasets demand similarly heavy capture and curation—EgoVerse 50K [30], for example, was assembled over  $\sim 1,500$  hours of in-person recording across many participants before any policy training could begin.

The language paired with these demonstrations does not face the same bottleneck. A typical clip is labeled with a short instruction such as “open the drawer” that names the goal but leaves implicit the spatial relations, contact transitions, embodiment state, and subgoal structure already present in the pixels and recorded actions. Re-annotating an existing dataset with richer descriptions costs orders of magnitude less than collecting new demonstrations: a single VLM call produces a multi-sentence caption in seconds at sub-cent cost and with no skilled human labor, while every new demonstration requires teleoperation time, dedicated hardware, and environment setup. We treat *language density* as a cheap lever for extracting more signal from a fixed demonstration dataset.

We instantiate this lever as **DeMiAn (Dense Multi-aspect Annotation)**, an end-to-end approach with two stages: a training-time pipeline that re-annotates existing demonstration videos along multiple aspects, and an inference-time *instructor* that supplies a task-appropriate aspect at deployment (§3). Whereas prior dense-language work in robotics commits to a single style of caption—motion primitives [3], step-level chain-of-thought [40], or captions used for representation pretraining [24, 17]—and uses it as a fixed training signal, we treat which aspect to use as a per-task design choice and learn to make that choice at deployment. The pipeline produces four aspects per segment—*physical motion*, *scene composition*, *arm pose*, and segment-level *reasoning*—each surfacing a distinct kind of structure that a one-line task label omits, and we apply it to 11K RoboCasa 365 clips [25, 26], a 1M-scale MolmoBot dataset [9], and 50K EgoVerse human-egocentric clips [30] without collecting any new demonstrations. Different aspects help different tasks (§4.1), so any fixed-aspect deployment would underperform an oracle that picks per task; the instructor learns—via supervised fine-tuning—to approximate the per-task oracle from an initial scene snapshot and runs asynchronously at no added latency, turning a fixed demonstration dataset into a per-task source of language signal at deployment.

We evaluate DeMiAn on two popular robot policy architectures: *DeMiAn VLA*, built on openpi 0.5 [5], and *DeMiAn WAM*, a video-based world-action model [29]. We first show that a small learned instructor closes most of the per-task oracle gap from a single scene snapshot, raising RoboCasa success rate by 5 percentage points over the no-annotation baseline and reaching within 3 points of the oracle (§4.2). The trained system extends to composite tasks and shows stronger OOD generalization on MolmoSpaces scenes and objects than the task-only baseline (§4.3). We further examine the compute-performance trade-off and find that dense annotation improves the frontier in both VLA post-training and WAM mid-training even after annotation-generation FLOPs are charged into the budget, making re-annotation a practical compute-efficient lever (§4.4).

Taken together, our contributions are: (i) an automatic VLM re-annotation pipeline that surfaces four aspects of structure latent in existing robot and human demonstrations; (ii) a learned *instructor*, trained via supervised fine-tuning and deployed asynchronously at no added latency, that closes

most of the per-task oracle gap from a single scene snapshot; (iii) empirical evidence that this combination generalizes beyond the atomic training distribution to composite tasks and OOD scenes; and (iv) a controlled compute-matched comparison showing that re-annotation improves the compute-performance frontier in both VLA post-training and WAM mid-training, even when annotation-generation FLOPs are charged into the budget. At 1M-clip MolmoBot scale, DeMiAn matches the no-annotation baseline on MolmoSpaces NextTo and Color with  $\sim 62\%$  less compute, positioning dense re-annotation as a complementary, compute-efficient lever alongside demonstration scaling.

## 2 Related Work

### 2.1 Language-Conditioned Robotic Manipulation

**Task-instruction conditioning.** A substantial body of work conditions robot policies on a single short language instruction. CLIPort [32] grounds instructions as pixel-wise affordances via CLIP [31] representations; BC-Z [15] conditions imitation learning on task descriptions for zero-shot generalization; VIMA [16] extends this to interleaved multimodal prompts. More recent vision-language-action (VLA) models scale this recipe dramatically: PaLM-E [10] injects embodied observations into a pretrained language model, while RT-2 [7] and OpenVLA [19] co-finetune vision-language backbones on internet-scale data and robot trajectories, producing policies that inherit broad semantic knowledge from pretraining.

**Sub-instruction language.** A few recent efforts introduce language at a finer temporal grain: RT-H [3] inserts “language motions” between tasks and actions, embodied chain-of-thought approaches [40] emit step-level reasoning before actions, and Ahn et al. [1] grounds LLM plans in learned affordances.

In most of these policies, language serves primarily as a *task identifier* (e.g., “pick up the apple”), with generalization evaluated by varying the instruction while holding the description style fixed; finer-grained variants like RT-H [3] and ECoT [40] relax this but each commits to a single fixed style of sub-instruction. Our work instead asks *what kind* of dense language best supports policy learning—pairing each training frame with one of four aspect-specific captions—and finds that the choice of caption type matters as much as its presence.

### 2.2 Dense Language Supervision and Reasoning for Embodied Agents

**Inference-time language reasoning.** A growing body of work leverages language-based reasoning in embodied settings at *inference time*. Chain-of-thought prompting [36] established that eliciting step-by-step reasoning substantially improves LLM performance on complex tasks. Inner Monologue [14] closes the loop around LLM planners by feeding environment language feedback back into the prompt. Code as Policies [22] and Language Models as Zero-Shot Planners [13] instead have LLMs emit executable programs or action sequences that invoke low-level robot skills. ProgPrompt [33] generates situated plans by combining LLM program synthesis with environment state assertions. Across this line of work, language reasoning guides high-level decision-making at test time; the low-level policy itself receives only a short task instruction.

**Training-time language supervision.** A complementary line of work uses language as a training signal rather than an inference-time aid. R3M [24] and Voltron [17] pretrain visual representations by aligning video frames with captions of human activity, producing features that transfer to downstream manipulation, and LIV [23] unifies language-image value learning and reward specification within a single pretraining objective. ROSIE [39] instead treats language as a data-augmentation interface, using text-to-image models to synthesize novel scenes from prompts and expand the visual diversity of robot training data. Thought Cloning [12] trains agents to generate natural-language thoughts while acting, using human think-aloud demonstrations as supervision.

Unlike prior work that uses language for representation pretraining or data augmentation, we provide dense per-step captions as an auxiliary co-training signal during VLA fine-tuning, with captions required only at training time. We further systematically vary the *type* of language supervision and find that the optimal caption type differs across manipulation primitives.

### 3 DeMiAn: Dense Multi-Aspect Annotation

DeMiAn amplifies the language signal in existing demonstrations without collecting new data through two stages: a training-time *annotation pipeline* that re-labels each video segment along multiple complementary aspects, and an inference-time *instructor* that selects an appropriate aspect per task at deployment. We describe each in turn below.

**Choice of annotation aspects.** Most language-supervised robot policies commit to a single sub-instruction style: motion primitives in RT-H [3], step-by-step chain-of-thought rationales in ECoT [40], scene and object grounding in CLIPort [32], or environment-state monologue in Inner Monologue [14]. Each style has been shown to help, but along a different axis of the manipulation problem. We consolidate these paradigms into four complementary annotation *aspects*—each a distinct dimension of the interaction described by its own caption—chosen to cover the structural information that a one-line task label leaves implicit (Table 1): `physical_motion` for temporal action and contact grounding, `scene_composition` for spatial grounding, `arm_pose` for embodiment and contact-state grounding, and `reasoning` for causal and subgoal grounding. Each segment is independently annotated along all four axes, so a downstream model can be trained on any single aspect, on a mixture, or with the aspect varying per segment.

Table 1: The four dense-annotation aspects used by DeMiAn. Each aspect targets and enriches information that is initially weakly specified by a one-line task description.

Annotation aspect	Motivation	Annotation signal
<code>physical_motion</code>	Temporal action and contact grounding.	Hand or end-effector motion: reaching, grasping, lifting, placing, opening, closing, and the objects involved.
<code>scene_composition</code>	Spatial grounding.	Workspace, visible objects, distractors, and task-relevant spatial relations.
<code>arm_pose</code>	Embodiment and contact-state grounding.	Hand or arm posture, reach direction, and contact state at segment boundaries.
<code>reasoning</code>	Causal and subgoal grounding.	Segment purpose (preparation, main manipulation, cleanup) and dependencies on neighboring segments.

**Annotation pipeline.** A *segment* is a contiguous sub-interval of an episode that the dataset metadata associates with a single one-line label (e.g., a frame range labeled “open the drawer”). For each segment, we sample up to  $F=10$  uniformly spaced frames and issue one VLM call per aspect  $k \in \mathcal{K} = \{\text{physical\_motion, scene\_composition, arm\_pose, reasoning}\}$ . Each call is conditioned on the sampled frames and a context block containing the task description, scene descriptor, object list, and neighboring segment labels; prompts enforce a strict JSON schema and a two-sentence length cap. The output is one caption per aspect for the segment.

We apply this pipeline to three existing datasets without collecting new demonstrations: RoboCasa 365 [25, 26], MolmoBot [9] (1M clips), and EgoVerse 50K [30]. RoboCasa atomic tasks can span multiple primitive motions, so we split long demonstrations into single-primitive clips before annotation (e.g., `OpenDoubleDoor` becomes two single-door clips); MolmoBot clips are short enough to annotate as-is. For EgoVerse, we recast the four aspects in human-egocentric language (hand motion and object transitions, egocentric workspace, observable hand/arm state, subgoal links); see Appendix A for the adapted prompts. The labeling model is Qwen3-VL-30B-A3B-Instruct [2].

**Learned Instructor.** The instructor is trained via supervised fine-tuning with reward-weighted target sampling. We first construct a reward table  $w(\tau, k)$  by running the action policy with each of the four GT fixed-aspect annotations across all training tasks and recording per-task validation SR. For each training episode, the target aspect is sampled from a softmax over  $w(\tau, \cdot)$  (temperature  $T=2$ , top-3 truncation), and the matching pipeline-generated caption is used as the SFT target. Tasks where every aspect underperforms the no-annotation baseline are assigned an empty target, teaching the instructor to abstain. Full details in Appendix C.2.

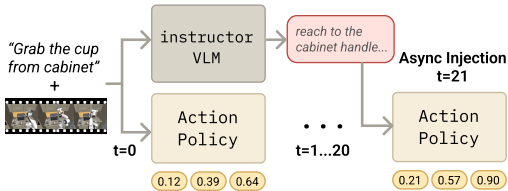


Figure 2: Asynchronous Instruction Injection.

Tasks where every aspect underperforms the no-annotation baseline are assigned an empty target, teaching the instructor to abstain. Full details in Appendix C.2.

At deployment, the generated annotation is concatenated with the task description and placed in the same prompt slot. The instructor runs *asynchronously* alongside the action policy: the robot begins acting with the task description alone, and the generated annotation is inserted at the next action-chunk boundary once it is ready (Figure 2). This hides instruction-generation latency behind the rollout and preserves the action server’s normal control cadence.

## 4 Experiments

Our experiments evaluate how DeMiAn improves and scales robot policy learning along four axes. We characterize how each annotation aspect affects per-task performance and quantify the per-task oracle gap (§4.1). We evaluate the trained instructor against that oracle (§4.2). We test generalization beyond the atomic training distribution to composite-task chaining and OOD scenes and objects (§4.3). We characterize how DeMiAn scales in WAM mid-training and VLA post-training relative to growing the demonstration dataset (§4.4).

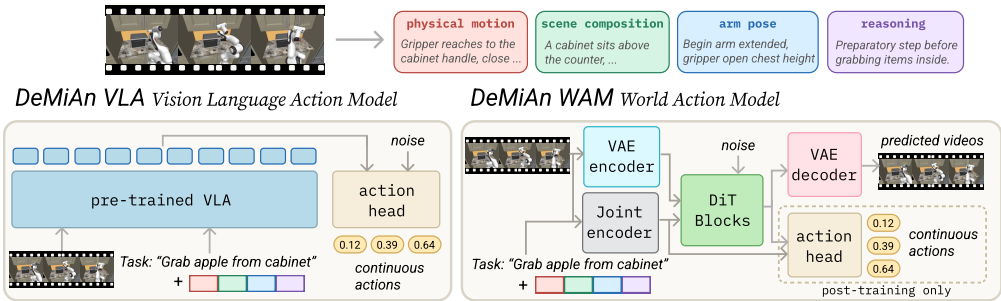


Figure 3: Overview of the policy-model architectures (DeMiAn VLA and DeMiAn WAM).

**Policy models.** Our experiments cover two representative robot policy architectures: vision-language-action policy (VLA) and world-model-based action policy (WAM), which span the mainstream paradigms in modern robot policy learning. VLAs inherit broad semantic priors from large-scale image-text pre-training; WAMs instead build their backbones from raw videos at scales far beyond robot teleoperation, enabling transfer across embodiments. Testing DeMiAn against both lets us investigate whether the language density lever is architecture-specific or generalizes across this language-conditioned / video-pretrained divide. We call the two architectures *DeMiAn VLA* and *DeMiAn WAM*, respectively, with details shown in Figure 3. **DeMiAn VLA:** We use the open-source `openpi 0.5` [5] as the VLA backbone, a PaliGemma vision-language backbone paired with a flow-matching action expert. Relative to the original `openpi`, we add a small annotation-level LM cross-entropy ( $\lambda_{LM} = 0.1$ ) as a regularizer rather than a generative objective, which prevents the bidirectional decoder from compressing the annotation into a coarse global summary. **DeMiAn WAM:** We follow prior work that adapts video-generative world models for robot control by decoding actions from their learned spatiotemporal representations [37, 20, 38] with a Cosmos-Predict 2.5 DiT backbone [29]. Unlike joint video-action denoising, the video objective is unchanged and actions are predicted deterministically from the learned video features. Across all annotation ablations the model architecture, visual data, and action targets are held fixed; only the language paired with each demonstration changes. Full training objective and the rationale are in Appendix B.1.

**Evaluation protocol.** We use two benchmark suites for evaluation: RoboCasa365 and MolmoSpaces. RoboCasa365 evaluation uses 17 atomic kitchen tasks in the held-out target split. MolmoSpaces bench-v2 [21] comprises nine benchmarks across four task families (Pick, Pick+Place (P+P), Pick+Place+NextTo, Pick+Place+Color) and varies difficulty along arm-initialization noise and scene distribution. We report success rate (SR) throughout. For RoboCasa365, given the task goal, an episode is successful if the simulator’s task checker returns success during the rollout. For MolmoSpaces, SR is evaluated on deterministic benchmark episodes and counts an episode successful if the task-specific success condition holds continuously for at least 0.5s at any point during the rollout. Episode counts, seeds, and full protocol details are in Appendix B.2.

Table 2: Success rate for training-time annotation ablations on RoboCasa365 and MolmoSpaces, grouped by policy architecture. Values are fractions in  $[0, 1]$ ; higher is better. Underlined values mark the per-column best among the five training-time annotation types (Baseline through Reasoning); **bold** values mark the per-column best across all rows including *w/ instructor*. The *Per-task Best (oracle)* row is excluded from this comparison. MolmoSpaces columns summarize Table 7: Pick and P+P average the Standard (Std) and Hard splits, NextTo uses In-Distribution (ID), Color is unchanged, and Avg. (in blue) averages these four family summaries.

Annotation aspect	RoboCasa365														MolmoSpaces								
	CloseBlenderLid	CloseFridge	CloseToasterOvenDoor	CoffeeSetupMug	OpenCabinet	OpenDrawer	OpenStandMixerHead	PnPCounterToCabinet	PnPCounterToStove	PnPDrawerToCounter	PnPSinkToCounter	PnPToasterToCounter	SlideDishwasherRack	TurnOffStove	TurnOnElectricKettle	TurnOnMicrowave	TurnOnSinkFaucet	Avg.	Pick (Avg of Std/Hard)	P+P (Avg of Std/Hard)	NextTo	Color	Avg.
<b>DeMiAn VLA</b>																							
Baseline (task-only)	.02	.65	.60	.29	.35	.10	<b>.84</b>	.53	.50	<u>.20</u>	<u>.76</u>	.55	.38	.05	<b>.86</b>	<u>.42</u>	<b>.43</b>	<u>.44</u>	.48	<b>.64</b>	.25	.41	<u>.44</u>
Physical Motion	<b>.03</b>	.63	<b>.74</b>	<b>.60</b>	.38	.12	<u>.76</u>	.61	<u>.58</u>	.15	.75	.59	<b>.75</b>	<b>.10</b>	.73	.18	.18	<u>.46</u>	.59	.60	.20	<u>.46</u>	<b>.46</b>
Scene Composition	.02	.64	.52	.46	<b>.42</b>	<u>.14</u>	<u>.77</u>	<b>.62</b>	.57	.10	.73	<u>.62</u>	.65	.08	.73	.26	.17	<u>.44</u>	<b>.61</b>	.60	.26	<u>.40</u>	<b>.47</b>
Arm Pose	<b>.03</b>	<b>.71</b>	.66	.32	<u>.38</u>	<u>.06</u>	.73	<u>.42</u>	.50	.15	.69	<u>.33</u>	.46	.05	.67	.07	.15	<u>.38</u>	.54	.60	.18	.45	<u>.44</u>
Reasoning	<b>.03</b>	.54	.40	.36	.26	.05	.72	.48	.52	.08	.62	.34	.50	.05	.66	.26	.40	<u>.37</u>	.59	.60	<b>.33</b>	.39	<u>.48</u>
w/ instructor	<b>.03</b>	.47	.55	.53	.41	<b>.47</b>	.80	.53	<b>.64</b>	<b>.21</b>	<b>.76</b>	<b>.72</b>	.55	<b>.10</b>	.72	<b>.48</b>	<b>.43</b>	<b>.49</b>	.60	.60	.27	<b>.48</b>	<b>.49</b>
Per-task Best (oracle)	.03	.71	.74	.60	.42	.14	.84	.62	.58	.20	.76	.62	.75	.10	.86	.42	.43	<u>.52</u>	.61	.64	.33	.46	<u>.51</u>
<b>DeMiAn WAM</b>																							
Baseline (task-only)	<b>.02</b>	.26	.16	.16	.12	<u>.06</u>	<b>.35</b>	.23	.22	.04	.26	<u>.25</u>	.27	<b>.06</b>	<u>.30</u>	<u>.13</u>	.14	<u>.18</u>	.26	.19	.06	.14	<u>.16</u>
Physical Motion	.01	.25	<b>.30</b>	<b>.24</b>	.15	.05	.30	.24	<b>.23</b>	<u>.06</u>	<b>.30</b>	.24	<b>.30</b>	.04	.29	.07	.07	<u>.18</u>	<u>.30</u>	<u>.21</u>	.07	<u>.15</u>	<u>.18</u>
Scene Composition	.01	.26	.21	.18	<u>.17</u>	<u>.06</u>	.31	<u>.25</u>	<b>.23</b>	.04	.29	<u>.25</u>	.26	.03	.29	.10	.07	<u>.18</u>	<u>.30</u>	.20	.09	<u>.13</u>	<u>.18</u>
Arm Pose	.01	<b>.28</b>	.26	.13	.15	.02	.29	.17	.20	<u>.06</u>	.28	.13	.18	.02	.27	.03	.06	<u>.15</u>	.25	.17	.06	<u>.15</u>	<u>.16</u>
Reasoning	.01	.22	.16	.14	.10	.02	.29	.19	.21	.03	.25	.14	.20	.02	.26	.10	<u>.16</u>	<u>.15</u>	.28	.19	<u>.11</u>	.13	<u>.18</u>
w/ instructor	<b>.02</b>	.14	.29	.10	<b>.19</b>	<b>.13</b>	.30	<b>.26</b>	.22	<b>.08</b>	.24	<b>.26</b>	.29	.05	<b>.32</b>	<b>.18</b>	<b>.18</b>	<b>.19</b>	<b>.31</b>	<b>.23</b>	.09	<b>.16</b>	<b>.20</b>
Per-task Best (oracle)	.02	.28	.30	.24	.17	.06	.35	.25	.23	.06	.30	.25	.30	.06	.30	.13	.16	<u>.20</u>	.30	.21	.11	.15	<u>.19</u>

#### 4.1 RQ1: Which annotation type works best for each task?

We train both action policies with each of the four annotation aspects independently and with the original task-only label (*Baseline*), and measure RoboCasa365 and MolmoSpaces SR at fixed compute. We also report a *Per-task Best (oracle)* row that takes the column-wise maximum across the annotation rows, an upper bound over fixed annotation aspects.

**The oracle gap.** Table 2 shows that dense annotation helps, but not uniformly. On RoboCasa with DeMiAn VLA, *Physical Motion* delivers large per-task lifts over the task-only baseline: *SlideDishwasherRack* jumps from 38% to 75% with Physical Motion, *CoffeeSetupMug* from 29% to 60%, and *CloseToasterOvenDoor* from 60% to 74%, while *Arm Pose* and *Reasoning* are markedly less useful. On MolmoSpaces, *Scene Composition* adds 13 percentage points on *Pick* tasks, and the *Reasoning* aspect improves 8 percentage points over the baseline in the *NextTo* task. Since no fixed aspect wins everywhere, we ask: *what if an oracle instructor could pick the right aspect for each task?* The per-task oracle reaches 52% Avg. SR, an 8 percentage point lift over the baseline and 6 percentage points above the best fixed aspect (*Physical Motion*, 46%). DeMiAn WAM shows the same shape at lower absolute SR (best fixed aspect 18%, oracle 20%). However, the oracle is unrealizable at deployment, where the right aspect is not known a priori—closing this gap is the goal of our learned instructor approach (§4.2).

**What does the model learn from dense annotation?** With the observation that some aspects can be dramatically helpful on specific tasks (e.g., 37 percentage points in *SlideDishwasherRack* with *Physical Motion*), we probe *what* the action modules are reading from the prompt by visualizing their attention over prefix tokens during rollouts and inspecting the resulting patterns across tasks. Figure 4 shows an example on *CloseToasterOvenDoor*. In the baseline policy, attention over prompt tokens is overwhelmingly concentrated on the <bos> token, with negligible weight on the task description that follows; the prompt is, in effect, being used as a position anchor rather than being read as language.

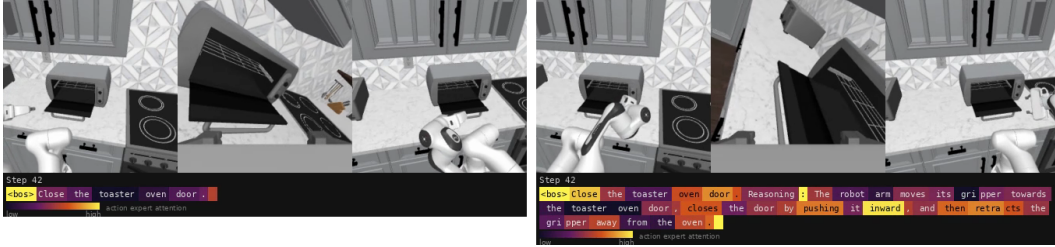


Figure 4: Action expert attention over prefix tokens at step 42 of a *CloseToasterOvenDoor* rollout. **Left:** task-only baseline—attention is collapsed onto the `<bos>` token, with the task description “Close the toaster oven door”. **Right:** policy trained with *Physical Motion* annotations—attention spreads across object mentions (*oven door*), motion verbs (*push*, *retracts*), and directional adverbs (*inward*, *away*) in the annotation, indicating that the action expert is actively reading the dense caption rather than the task label alone.

In the Physical-Motion-annotated policy, attention instead distributes across linguistically grounded units of the annotation: interacting objects (“*oven door*”), motion verbs not present in the task label (“*push*”, “*retracts*”), and directional adverbs (“*inward*”, “*away*”).

**Implication.** No fixed annotation rule reaches the per-task oracle. Per-task and per-family breakdowns—which aspect wins on which task, where the baseline is strongest, and how the patterns differ on RoboCasa vs MolmoSpaces—are deferred to Appendix C.1. The optimal aspect varies with the structural demands of each task family (contact-changing motion vs. open-vocabulary grounding); closing this gap requires producing the right instruction for each task at deployment, which is precisely what RQ2 evaluates.

## 4.2 RQ2: Can a learned instructor approach the per-task oracle?

Our analysis shows that no fixed annotation rule reaches the per-task oracle, and that the optimal aspect varies with the structural demands of each task family. We close this gap with a small learned *instructor* model: given the same observation the action policy receives, it generates a scene-grounded annotation. We use Qwen3.5-2B [34] as the instructor model. To make the action policy robust to whichever annotation the instructor emits at inference, we train it on prompts sampled uniformly across five conditions: the four DeMiAn aspects and the task-only baseline. At inference the instructor consumes (i) three RGB camera frames from the initial observation of the rollout and (ii) the natural-language task description. The output is concatenated to the task description and provided to the action policy as the conditioning prompt, occupying the same prompt slot used in § 4.1.

**Instructor closes the oracle gap.** The instructor raises average SR from 44% to 49% on RoboCasa and MolmoSpaces (Table 2), within 2–3 points of the per-task oracle (51–52%). To isolate the instructor’s contribution, we compare against a random per-episode aspect baseline (46.6% from Table 8) with the same action policy checkpoint: the instructor adds +3.8 points, indicating that the gain comes from learned per-task selection rather than heuristic routing alone. Comparisons with fixed-aspect GT injection are in Appendix C.2; per-task and per-family analyses are in Appendix C.1.

**Async deployment introduces no policy delay.** We test async deployment for real-time applications. At test time the instructor decodes asynchronously while actions emit at the action server’s native 8-step open-loop cadence. Until the instruction is ready, the policy executes on the task description alone, equivalent to the no-annotation baseline; the moment the instruction completes it is spliced into the reasoning field at the next chunk boundary, and subsequent action chunks condition on it.

We compare this design against a *synchronous* variant that blocks the first action until the instruction completes (Table 3). Async tracks sync within fractional points on SR (49.0% vs 49.5%) while injecting the instruction into a rollout already in progress: the policy never waits for the instructor, and the  $\sim 1.87$  s of generation latency is hidden behind the first  $\sim 22$  action steps.

Table 3: Async vs. sync instruction delivery comparison. *Mean injected step* is the action step at which the instruction first reaches the policy. *Mean injected time* is the mean wall-clock generation latency of the instructor for the same requests; in sync mode this latency directly delays the policy, whereas in async mode it overlaps with action execution and is therefore not added to rollout wall-clock.

Mode	Success Rate	Mean/Median injected step	Mean/Median injected time (s)
Sync Instructor	49.5%	1	0
Async Instructor	49.0%	21.9/23	1.87/1.86

### 4.3 RQ3: Does the method generalize on new instructions beyond the training distribution?

Our policy models are trained on the RoboCasa365 atomic tasks. We test generalization to new instruction formats on composite tasks. We curate 18 composite tasks, each composed of atomic tasks seen during training, so chaining the atomic-task policies should in principle suffice. We evaluate two prompting strategies to see how the action policy generalizes *unseen instructions*. *-fix* feeds a single composite task description for the whole episode; *-dynamic* runs a subgoal-driven state machine that swaps the prompt to the in-distribution atomic instruction for the current phase once a lenient in-simulator trigger fires. This yields four base configurations (*baseline-fix*, *baseline-dynamic*, *ours-fix*, *ours-dynamic*) where GT instructions are available at test time; we additionally evaluate *ours-dynamic-instructor*, which replaces the GT atomic prompt with the DeMiAn instructor’s output and tests the full method end-to-end.

Table 4 illustrates the difference on *PrepareCoffee*: *-fix* feeds a single composite description across the entire episode, while *-dynamic* swaps the prompt to the in-distribution atomic instruction for the current phase. Each (task, config) is evaluated over 20 episodes with `max_steps=1200`. We report phase-*k* SR (fraction of episodes whose subgoal checker reaches the *k*-th milestone) and full-task SR via RoboCasa’s strict success-goal condition checker.

Table 4: Example of prompting for RoboCasa365 Composite task *PrepareCoffee* (3-phase composite: pick mug → place under dispenser → press start). *-fix* provides one composite-task description for the entire episode. *-dynamic* swaps to the atomic instruction for the current phase, triggered when the policy’s done-flag exceeds threshold and a lenient in-simulator condition fires.

Mode	Phase 1	Phase 2	Phase 3
<i>-fix</i>	Pick up the mug from the cabinet, place it under the coffee machine dispenser, then press the start button to brew coffee.		
<i>-dynamic</i>	Pick up the mug from the cabinet.	Place the mug under the coffee machine dispenser.	Press the start button on the coffee machine.

Table 5: Composite-task results on 18 RoboCasa365 composites. Phase-*k* SR counts episodes that reach the *k*-th subgoal milestone.

Metric	<i>-fix</i>		<i>-dynamic</i>		
	Baseline	DeMiAn-VLA	Baseline (GT)	DeMiAn-VLA (GT)	DeMiAn-VLA (instr.)
Mean phase-1 SR	50%	52%	57%	<b>65%</b>	61%
Mean phase-2 SR	28%	<b>32%</b>	26%	31%	30%
Mean full-task SR	13%	15%	19%	<b>22%</b>	18%

Table 5 shows the results of the composite-task chaining experiment. First, within the OOD *-fix* format, DeMiAn-VLA improves over the task-only baseline by +2 full-task points (15% vs 13%), suggesting that dense annotations yield modest robustness to instruction formats outside training. Second, with GT atomic prompts under *-dynamic*, DeMiAn-VLA-GT is the strongest configuration overall (22% vs 19% baseline-GT), showing that the dense-annotation policy benefits more from subgoal-decomposed prompts than the baseline does. Third, replacing the GT atomic prompt with the DeMiAn instructor at deployment recovers most but not all of this benefit: full-task SR drops to 18%, sitting between the two GT configurations and approximately 1 point below baseline-GT.

The instructor still leads on Phase-1 and Phase-2 milestones (61%/30% vs 57%/26%), so the gap concentrates in the final phase. Closing this last-phase gap is left for future work.

#### 4.4 RQ4: Is dense annotation a compute-efficient lever?

We ask whether the upfront cost of generating dense annotations is recovered by training-time gains, charging caption-generation FLOPs into the compute budget. Gao et al. [11] show that a video-generative backbone trained on human video alone—without any robot action labels—transfers usefully to downstream robot manipulation. We refer to training a video-generative backbone with human video as the *mid-training* stage, in contrast to the *post-training* stage where an action head is attached to the backbone and robot action data are available. We evaluate the effect of DeMiAn across both mid-training and post-training stages. We first mid-train DeMiAn WAM on 50K human-egocentric clips from EgoVerse [30] with no action head attached, optimized purely on a video-prediction objective; the DeMiAn annotations enter as language conditioning on the video model.

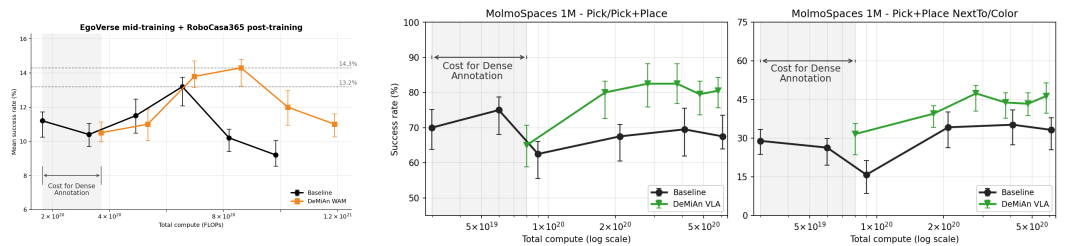


Figure 5: **DeMiAn under scaling.** (A) DeMiAn-WAM mid-training on EgoVerse 50K with dense annotations, evaluated on downstream RoboCasa 365. The x-axis includes both mid-training compute and annotation-generation compute. (B) DeMiAn-VLA post-training on the 1M-scale MolmoBot corpus, evaluated by total success across four MolmoSpaces benchmarks. The x-axis includes annotation-generation and DeMiAn-VLA post-training FLOPs.

**Scaling under matched compute.** We mid-train the Cosmos-Predict 2.5 model on 50K EgoVerse clips with and without dense annotations and post-train DeMiAn-WAM on RoboCasa365 under both conditions. Figure 5 reports both regimes with annotation-generation compute charged into the x-axis. After the small upfront cost of generating annotations, the annotated WAM reaches higher downstream RoboCasa SR than the baseline at nearby compute budgets (Fig. 5A). On MolmoBot post-training with 1M trajectories, annotation-conditioned policies reach stronger MolmoSpaces SR earlier in training and obtain higher peak performance than the task-only baseline (Fig. 5B). On the MolmoSpaces NextTo and Color tasks, DeMiAn matches the no-annotation baseline with  $\sim 62\%$  less compute, saving  $\sim 1.3 \times 10^{20}$  FLOPs.

**Annotation cost.** A single Qwen3-VL-30B call processes  $\approx 8.2K$  input tokens (frames + prompt) and emits  $\approx 150$  output tokens, costing  $\approx \$1.1 \times 10^{-3}$  on hosted inference. For a 1M-clip MolmoBot corpus with one DeMiAn aspect per clip, this totals  $5.0e19$  FLOPs; see Appendix A.3 for the calculation.

**Implication.** At fixed compute, dense annotation accelerates both WAM mid-training and VLA post-training even after charging caption-generation compute against the budget. Combined with the cost asymmetry above, this confirms that adding language to existing demonstrations is a practical and compute-efficient lever in robot policy learning.

## 5 Conclusion

We studied dense, structured language as a supervision channel for robot policy learning, treating annotation *type* as a first-class design choice rather than a fixed prompt format. Our automatic VLM-based pipeline produces four complementary annotation channels—physical motion, scene composition, arm pose, and reasoning—across robot teleoperation and human-egocentric video, spanning RoboCasa 365, MolmoBot, and EgoVerse.

Three findings emerge from this study. First, dense language improves robot manipulation, but the *best* channel is task-dependent: action-, scene-, pose-, and reasoning-style annotations help different task families differently, and a per-task oracle reliably exceeds any single fixed choice. Second, the benefit persists as training scales: dense annotations improve the compute-performance trade-off in both WAM mid-training on EgoVerse and VLA post-training on the 1M-scale MolmoBot corpus, even after charging annotation-generation compute against the budget. Third, dense language is deployable: a small asynchronous instructor closes most of the oracle gap at inference time, and annotation-trained policies generalize to long-horizon composite tasks when paired with subgoal-driven prompt switching.

## References

- [1] Michael Ahn, Anthony Brohan, Noah Brown, Yevgen Chebotar, Omar Cortes, Byron David, Chelsea Finn, Chuyuan Fu, Keerthana Gopalakrishnan, Karol Hausman, Alex Herzog, Daniel Ho, Jasmine Hsu, Julian Ibarz, Brian Ichter, Alex Irpan, Eric Jang, Rosario Jauregui Ruano, Kyle Jeffrey, Sally Jesmonth, Nikhil J Joshi, Ryan Julian, Dmitry Kalashnikov, Yuheng Kuang, Kuang-Huei Lee, Sergey Levine, Yao Lu, Linda Luu, Carolina Parada, Peter Pastor, Jornell Quiambao, Kanishka Rao, Jarek Rettinghouse, Diego Reyes, Pierre Sermanet, Nicolas Sievers, Clayton Tan, Alexander Toshev, Vincent Vanhoucke, Fei Xia, Ted Xiao, Peng Xu, Sichun Xu, Mengyuan Yan, and Andy Zeng. Do as i can, not as i say: Grounding language in robotic affordances, 2022. URL <https://arxiv.org/abs/2204.01691>.
- [2] Shuai Bai, Yuxuan Cai, Ruizhe Chen, Keqin Chen, Xionghui Chen, Zesen Cheng, Lianghao Deng, Wei Ding, Chang Gao, Chunjiang Ge, Wenbin Ge, Zhifang Guo, Qidong Huang, Jie Huang, Fei Huang, Binyuan Hui, Shutong Jiang, Zhaohai Li, Mingsheng Li, Mei Li, Kaixin Li, Zicheng Lin, Junyang Lin, Xuejing Liu, Jiawei Liu, Chenglong Liu, Yang Liu, Dayiheng Liu, Shixuan Liu, Dunjie Lu, Ruilin Luo, Chenxu Lv, Rui Men, Lingchen Meng, Xuancheng Ren, Xingzhang Ren, Sibao Song, Yuchong Sun, Jun Tang, Jianhong Tu, Jianqiang Wan, Peng Wang, Pengfei Wang, Qiuyue Wang, Yuxuan Wang, Tianbao Xie, Yiheng Xu, Haiyang Xu, Jin Xu, Zhibo Yang, Mingkun Yang, Jianxin Yang, An Yang, Bowen Yu, Fei Zhang, Hang Zhang, Xi Zhang, Bo Zheng, Humen Zhong, Jingren Zhou, Fan Zhou, Jing Zhou, Yuanzhi Zhu, and Ke Zhu. Qwen3-vl technical report, 2025. URL <https://arxiv.org/abs/2511.21631>.
- [3] Suneel Belkhole, Tianli Ding, Ted Xiao, Pierre Sermanet, Quon Vuong, Jonathan Tompson, Yevgen Chebotar, Debidatta Dwibedi, and Dorsa Sadigh. Rt-h: Action hierarchies using language, 2024. URL <https://arxiv.org/abs/2403.01823>.
- [4] Kevin Black, Noah Brown, James Darpinian, Karan Dhabalia, Danny Driess, Adnan Esmail, Michael Robert Equi, Chelsea Finn, Niccolo Fusai, Manuel Y. Galliker, Dibya Ghosh, Lachy Groom, Karol Hausman, brian ichter, Szymon Jakubczak, Tim Jones, Liyiming Ke, Devin LeBlanc, Sergey Levine, Adrian Li-Bell, Mohith Mothukuri, Suraj Nair, Karl Pertsch, Allen Z. Ren, Lucy Xiaoyang Shi, Laura Smith, Jost Tobias Springenberg, Kyle Stachowicz, James Tanner, Quan Vuong, Homer Walke, Anna Walling, Haohuan Wang, Lili Yu, and Ury Zhilinsky.  $\pi_{0.5}$ : a vision-language-action model with open-world generalization. In Joseph Lim, Shuran Song, and Hae-Won Park, editors, *Proceedings of The 9th Conference on Robot Learning*, volume 305 of *Proceedings of Machine Learning Research*, pages 17–40. PMLR, 27–30 Sep 2025. URL <https://proceedings.mlr.press/v305/black25a.html>.
- [5] Kevin Black, Noah Brown, Danny Driess, Adnan Esmail, Michael Equi, Chelsea Finn, Niccolo Fusai, Lachy Groom, Karol Hausman, Brian Ichter, Szymon Jakubczak, Tim Jones, Liyiming Ke, Sergey Levine, Adrian Li-Bell, Mohith Mothukuri, Suraj Nair, Karl Pertsch, Lucy Xiaoyang Shi, James Tanner, Quan Vuong, Anna Walling, Haohuan Wang, and Ury Zhilinsky.  $\pi_0$ : A vision-language-action flow model for general robot control, 2026. URL <https://arxiv.org/abs/2410.24164>.
- [6] Anthony Brohan, Noah Brown, Justice Carbajal, Yevgen Chebotar, Joseph Dabis, Chelsea Finn, Keerthana Gopalakrishnan, Karol Hausman, Alexander Herzog, Jasmine Hsu, Julian Ibarz, Brian Ichter, Alex Irpan, Tomas Jackson, Sally Jesmonth, Nikhil J. Joshi, Ryan C. Julian, Dmitry Kalashnikov, Yuheng Kuang, Isabel Leal, Kuang-Huei Lee, Sergey Levine, Yao Lu, Utsav Malla, Deeksha Manjunath, Igor Mordatch, Ofir Nachum, Carolina Parada, Jodilyn Peralta, Emily Perez, Karl Pertsch, Jornell Quiambao, Kanishka Rao, Michael S. Ryoo, Grecia Salazar, Pannag R. Sanketi, Kevin Sayed, Jaspiar Singh, Sumedh Anand Sontakke, Austin Stone, Clayton Tan, Huong Tran, Vincent Vanhoucke, Steve Vega, Quan Ho Vuong, F. Xia, Ted Xiao, Peng Xu, Sichun Xu, Tianhe Yu, and Brianna Zitkovich. Rt-1: Robotics transformer for real-world control at scale. *ArXiv*, abs/2212.06817, 2022. URL <https://api.semanticscholar.org/CorpusID:254591260>.
- [7] Anthony Brohan, Noah Brown, Justice Carbajal, Yevgen Chebotar, Xi Chen, Krzysztof Choromanski, Tianli Ding, Danny Driess, Avinava Dubey, Chelsea Finn, Pete Florence, Chuyuan Fu, Montse Gonzalez Arenas, Keerthana Gopalakrishnan, Kehang Han, Karol Hausman, Alexander Herzog, Jasmine Hsu, Brian

- Ichter, Alex Irpan, Nikhil Joshi, Ryan Julian, Dmitry Kalashnikov, Yuheng Kuang, Isabel Leal, Lisa Lee, Tsang-Wei Edward Lee, Sergey Levine, Yao Lu, Henryk Michalewski, Igor Mordatch, Karl Pertsch, Kanishka Rao, Krista Reymann, Michael Ryoo, Grecia Salazar, Pannag Sanketi, Pierre Sermanet, Jaspiar Singh, Anikait Singh, Radu Soricut, Huong Tran, Vincent Vanhoucke, Quan Vuong, Ayzaan Wahid, Stefan Welker, Paul Wohlhart, Jialin Wu, Fei Xia, Ted Xiao, Peng Xu, Sichun Xu, Tianhe Yu, and Brianna Zitkovich. Rt-2: Vision-language-action models transfer web knowledge to robotic control, 2023. URL <https://arxiv.org/abs/2307.15818>.
- [8] Open X-Embodiment Collaboration, Abby O’Neill, Abdul Rehman, Abhinav Gupta, Abhiram Maddukuri, Abhishek Gupta, Abhishek Padalkar, Abraham Lee, Acorn Pooley, Agrim Gupta, Ajay Mandekar, Ajinkya Jain, Albert Tung, Alex Bewley, Alex Herzog, Alex Irpan, Alexander Khazatsky, Anant Rai, Anchit Gupta, Andrew Wang, Andrey Kolobov, Anikait Singh, Animesh Garg, Aniruddha Kembhavi, Annie Xie, Anthony Brohan, Antonin Raffin, Archit Sharma, Arefeh Yavary, Arhan Jain, Ashwin Balakrishna, Ayzaan Wahid, Ben Burgess-Limerick, Beomjoon Kim, Bernhard Schölkopf, Blake Wulfe, Brian Ichter, Cewu Lu, Charles Xu, Charlotte Le, Chelsea Finn, Chen Wang, Chenfeng Xu, Cheng Chi, Chenguang Huang, Christine Chan, Christopher Agia, Chuer Pan, Chuyuan Fu, Coline Devin, Danfei Xu, Daniel Morton, Danny Driess, Daphne Chen, Deepak Pathak, Dhruv Shah, Dieter Büchler, Dinesh Jayaraman, Dmitry Kalashnikov, Dorsa Sadigh, Edward Johns, Ethan Foster, Fangchen Liu, Federico Ceola, Fei Xia, Feiyu Zhao, Felipe Vieira Frujeri, Freek Stulp, Gaoyue Zhou, Gaurav S. Sukhatme, Gautam Salhotra, Ge Yan, Gilbert Feng, Giulio Schiavi, Glen Berseth, Gregory Kahn, Guangwen Yang, Guanzhi Wang, Hao Su, Hao-Shu Fang, Haochen Shi, Henghui Bao, Heni Ben Amor, Henrik I Christensen, Hiroki Furuta, Homanga Bharadhwaj, Homer Walke, Hongjie Fang, Huy Ha, Igor Mordatch, Ilija Radosavovic, Isabel Leal, Jacky Liang, Jad Abou-Chakra, Jaehyung Kim, Jaimyn Drake, Jan Peters, Jan Schneider, Jasmine Hsu, Jay Vakil, Jeannette Bohg, Jeffrey Bingham, Jeffrey Wu, Jensen Gao, Jiaheng Hu, Jiajun Wu, Jialin Wu, Jiankai Sun, Jianlan Luo, Jiayuan Gu, Jie Tan, Jihoon Oh, Jimmy Wu, Jingpei Lu, Jingyun Yang, Jitendra Malik, João Silvério, Joey Hejna, Jonathan Booher, Jonathan Tompson, Jonathan Yang, Jordi Salvador, Joseph J. Lim, Junhyek Han, Kaiyuan Wang, Kanishka Rao, Karl Pertsch, Karol Hausman, Keegan Go, Keerthana Gopalakrishnan, Ken Goldberg, Kendra Byrne, Kenneth Oslund, Kento Kawaharazuka, Kevin Black, Kevin Lin, Kevin Zhang, Kiana Ehsani, Kiran Lekkala, Kirsty Ellis, Krishan Rana, Krishnan Srinivasan, Kuan Fang, Kunal Pratap Singh, Kuo-Hao Zeng, Kyle Hatch, Kyle Hsu, Laurent Itti, Lawrence Yunliang Chen, Lerrel Pinto, Li Fei-Fei, Liam Tan, Linxi "Jim" Fan, Lionel Ott, Lisa Lee, Luca Weihs, Magnum Chen, Marion Lepert, Marius Memmel, Masayoshi Tomizuka, Masha Itkina, Mateo Guaman Castro, Max Spero, Maximilian Du, Michael Ahn, Michael C. Yip, Mingtong Zhang, Mingyu Ding, Minh Heo, Mohan Kumar Srirama, Mohit Sharma, Moo Jin Kim, Muhammad Zubair Irshad, Naoaki Kanazawa, Nicklas Hansen, Nicolas Heess, Nikhil J Joshi, Niko Suenderhauf, Ning Liu, Norman Di Palo, Nur Muhammad Mahi Shafiullah, Oier Mees, Oliver Kroemer, Osbert Bastani, Pannag R Sanketi, Patrick "Tree" Miller, Patrick Yin, Paul Wohlhart, Peng Xu, Peter David Fagan, Peter Mitrano, Pierre Sermanet, Pieter Abbeel, Priya Sundaesan, Qiuyu Chen, Quan Vuong, Rafael Rafailov, Ran Tian, Ria Doshi, Roberto Mart’in-Mart’in, Rohan Bajjal, Rosario Scalise, Rose Hendrix, Roy Lin, Runjia Qian, Ruohan Zhang, Russell Mendonca, Rutav Shah, Ryan Hoque, Ryan Julian, Samuel Bustamante, Sean Kirmani, Sergey Levine, Shan Lin, Sherry Moore, Shikhar Bahl, Shivin Dass, Shubham Sonawani, Shubham Tulsiani, Shuran Song, Sichun Xu, Siddhant Halder, Siddharth Karamcheti, Simeon Adebola, Simon Guist, Soroush Nasiriany, Stefan Schaal, Stefan Welker, Stephen Tian, Subramanian Ramamoorthy, Sudeep Dasari, Suneel Belkhal, Sungjae Park, Suraj Nair, Suvir Mirchandani, Takayuki Osa, Tanmay Gupta, Tatsuya Harada, Tatsuya Matsushima, Ted Xiao, Thomas Kollar, Tianhe Yu, Tianli Ding, Todor Davchev, Tony Z. Zhao, Travis Armstrong, Trevor Darrell, Trinity Chung, Vidhi Jain, Vikash Kumar, Vincent Vanhoucke, Vitor Guizilini, Wei Zhan, Wenxuan Zhou, Wolfram Burgard, Xi Chen, Xiangyu Chen, Xiaolong Wang, Xinghao Zhu, Xinyang Geng, Xiyuan Liu, Xu Liangwei, Xuanlin Li, Yansong Pang, Yao Lu, Yecheng Jason Ma, Yejin Kim, Yevgen Chebotar, Yifan Zhou, Yifeng Zhu, Yilin Wu, Ying Xu, Yixuan Wang, Yonatan Bisk, Yongqiang Dou, Yoonyoung Cho, Youngwoon Lee, Yuchen Cui, Yue Cao, Yueh-Hua Wu, Yujin Tang, Yuke Zhu, Yunchu Zhang, Yunfan Jiang, Yunshuang Li, Yunzhu Li, Yusuke Iwasawa, Yutaka Matsuo, Zehan Ma, Zhuo Xu, Zichen Jeff Cui, Zichen Zhang, Zipeng Fu, and Zipeng Lin. Open X-Embodiment: Robotic learning datasets and RT-X models. <https://arxiv.org/abs/2310.08864>, 2023.
- [9] Abhay Deshpande, Maya Guru, Rose Hendrix, Snehal Jauhri, Ainaz Eftekhari, Rohun Tripathi, Max Argus, Jordi Salvador, Haoquan Fang, Matthew Wallingford, Wilbert Pumacay, Yejin Kim, Quinn Pfeifer, Ying-Chun Lee, Piper Wolters, Omar Rayyan, Mingtong Zhang, Jiafei Duan, Karen Farley, Winson Han, Eli Vanderbilt, Dieter Fox, Ali Farhadi, Georgia Chalvatzaki, Dhruv Shah, and Ranjay Krishna. Molmob0t: Large-scale simulation enables zero-shot manipulation, 2026. URL <https://arxiv.org/abs/2603.16861>.
- [10] Danny Driess, Fei Xia, Mehdi S. M. Sajjadi, Corey Lynch, Aakanksha Chowdhery, Brian Ichter, Ayzaan Wahid, Jonathan Tompson, Quan Vuong, Tianhe Yu, Wenlong Huang, Yevgen Chebotar, Pierre Sermanet, Daniel Duckworth, Sergey Levine, Vincent Vanhoucke, Karol Hausman, Marc Toussaint, Klaus Greff, Andy Zeng, Igor Mordatch, and Pete Florence. Palm-e: An embodied multimodal language model, 2023. URL <https://arxiv.org/abs/2303.03378>.

- [11] Shenyuan Gao, William Liang, Kaiyuan Zheng, Ayaan Malik, Seonghyeon Ye, Sihyun Yu, Wei-Cheng Tseng, Yuzhu Dong, Kaichun Mo, Chen-Hsuan Lin, Qianli Ma, Seungjun Nah, Loic Magne, Jiannan Xiang, Yuqi Xie, Ruijie Zheng, Dantong Niu, You Liang Tan, K. R. Zentner, George Kurian, Suneel Indupuru, Pooya Jannaty, Jinwei Gu, Jun Zhang, Jitendra Malik, Pieter Abbeel, Ming-Yu Liu, Yuke Zhu, Joel Jang, and Linxi "Jim" Fan. Dreamdojo: A generalist robot world model from large-scale human videos, 2026. URL <https://arxiv.org/abs/2602.06949>.
- [12] Shengran Hu and Jeff Clune. Thought cloning: Learning to think while acting by imitating human thinking, 2024. URL <https://arxiv.org/abs/2306.00323>.
- [13] Wenlong Huang, Pieter Abbeel, Deepak Pathak, and Igor Mordatch. Language models as zero-shot planners: Extracting actionable knowledge for embodied agents, 2022. URL <https://arxiv.org/abs/2201.07207>.
- [14] Wenlong Huang, Fei Xia, Ted Xiao, Harris Chan, Jacky Liang, Pete Florence, Andy Zeng, Jonathan Tompson, Igor Mordatch, Yevgen Chebotar, Pierre Sermanet, Noah Brown, Tomas Jackson, Linda Luu, Sergey Levine, Karol Hausman, and Brian Ichter. Inner monologue: Embodied reasoning through planning with language models, 2022. URL <https://arxiv.org/abs/2207.05608>.
- [15] Eric Jang, Alex Irpan, Mohi Khansari, Daniel Kappler, Frederik Ebert, Corey Lynch, Sergey Levine, and Chelsea Finn. Bc-z: Zero-shot task generalization with robotic imitation learning, 2022. URL <https://arxiv.org/abs/2202.02005>.
- [16] Yunfan Jiang, Agrim Gupta, Zichen Zhang, Guanzhi Wang, Yongqiang Dou, Yanjun Chen, Li Fei-Fei, Anima Anandkumar, Yuke Zhu, and Linxi Fan. Vima: General robot manipulation with multimodal prompts, 2023. URL <https://arxiv.org/abs/2210.03094>.
- [17] Siddharth Karamcheti, Suraj Nair, Annie S. Chen, Thomas Kollar, Chelsea Finn, Dorsa Sadigh, and Percy Liang. Language-driven representation learning for robotics, 2023. URL <https://arxiv.org/abs/2302.12766>.
- [18] Alexander Khazatsky, Karl Pertsch, Suraj Nair, Ashwin Balakrishna, Sudeep Dasari, Siddharth Karamcheti, Soroush Nasiriany, Mohan Kumar Srirama, Lawrence Yunliang Chen, Kirsty Ellis, Peter David Fagan, Joey Hejna, Masha Itkina, Marion Lepert, Yecheng Jason Ma, Patrick Tree Miller, Jimmy Wu, Suneel Belkhale, Shivin Dass, Huy Ha, Arhan Jain, Abraham Lee, Youngwoon Lee, Marius Memmel, Sungjae Park, Ilija Radosavovic, Kaiyuan Wang, Albert Zhan, Kevin Black, Cheng Chi, Kyle Beltran Hatch, Shan Lin, Jingpei Lu, Jean Mercat, Abdul Rehman, Pannag R Sanketi, Archit Sharma, Cody Simpson, Quan Vuong, Homer Rich Walke, Blake Wulfe, Ted Xiao, Jonathan Heewon Yang, Arefeh Yavary, Tony Z. Zhao, Christopher Agia, Rohan Bajjal, Mateo Guaman Castro, Daphne Chen, Qiuyu Chen, Trinity Chung, Jaimyn Drake, Ethan Paul Foster, Jensen Gao, Vitor Guizilini, David Antonio Herrera, Minh Heo, Kyle Hsu, Jiaheng Hu, Muhammad Zubair Irshad, Donovan Jackson, Charlotte Le, Yunshuang Li, Kevin Lin, Roy Lin, Zehan Ma, Abhiram Maddukuri, Suvir Mirchandani, Daniel Morton, Tony Nguyen, Abigail O'Neill, Rosario Scalise, Derick Seale, Victor Son, Stephen Tian, Emi Tran, Andrew E. Wang, Yilin Wu, Annie Xie, Jingyun Yang, Patrick Yin, Yunchu Zhang, Osbert Bastani, Glen Berseth, Jeannette Bohg, Ken Goldberg, Abhinav Gupta, Abhishek Gupta, Dinesh Jayaraman, Joseph J Lim, Jitendra Malik, Roberto Martín-Martín, Subramanian Ramamoorthy, Dorsa Sadigh, Shuran Song, Jiajun Wu, Michael C. Yip, Yuke Zhu, Thomas Kollar, Sergey Levine, and Chelsea Finn. Droid: A large-scale in-the-wild robot manipulation dataset, 2025. URL <https://arxiv.org/abs/2403.12945>.
- [19] Moo Jin Kim, Karl Pertsch, Siddharth Karamcheti, Ted Xiao, Ashwin Balakrishna, Suraj Nair, Rafael Rafailov, Ethan Foster, Grace Lam, Pannag Sanketi, Quan Vuong, Thomas Kollar, Benjamin Burchfiel, Russ Tedrake, Dorsa Sadigh, Sergey Levine, Percy Liang, and Chelsea Finn. Openvla: An open-source vision-language-action model, 2024. URL <https://arxiv.org/abs/2406.09246>.
- [20] Moo Jin Kim, Yihuai Gao, Tsung-Yi Lin, Yen-Chen Lin, Yunhao Ge, Grace Lam, Percy Liang, Shuran Song, Ming-Yu Liu, Chelsea Finn, and Jinwei Gu. Cosmos policy: Fine-tuning video models for visuomotor control and planning, 2026. URL <https://arxiv.org/abs/2601.16163>.
- [21] Yejin Kim, Wilbert Pumacay, Omar Rayyan, Max Argus, Winson Han, Eli VanderBilt, Jordi Salvador, Abhay Deshpande, Rose Hendrix, Snehal Jauhri, Shuo Liu, Nur Muhammad Mahi Shafiullah, Maya Guru, Ainaz Eftekhari, Karen Farley, Donovan Clay, Jiafei Duan, Arjun Guru, Piper Wolters, Alvaro Herrasti, Ying-Chun Lee, Georgia Chalvatzaki, Yuchen Cui, Ali Farhadi, Dieter Fox, and Ranjay Krishna. Molmospaces: A large-scale open ecosystem for robot navigation and manipulation, 2026. URL <https://arxiv.org/abs/2602.11337>.
- [22] Jacky Liang, Wenlong Huang, Fei Xia, Peng Xu, Karol Hausman, Brian Ichter, Pete Florence, and Andy Zeng. Code as policies: Language model programs for embodied control, 2023. URL <https://arxiv.org/abs/2209.07753>.

- [23] Yecheng Jason Ma, William Liang, Vaidehi Som, Vikash Kumar, Amy Zhang, Osbert Bastani, and Dinesh Jayaraman. Liv: Language-image representations and rewards for robotic control, 2023. URL <https://arxiv.org/abs/2306.00958>.
- [24] Suraj Nair, Aravind Rajeswaran, Vikash Kumar, Chelsea Finn, and Abhinav Gupta. R3m: A universal visual representation for robot manipulation, 2022. URL <https://arxiv.org/abs/2203.12601>.
- [25] Soroush Nasiriany, Abhiram Maddukuri, Lance Zhang, Adeet Parikh, Aaron Lo, Abhishek Joshi, Ajay Mandlekar, and Yuke Zhu. Robocasa: Large-scale simulation of everyday tasks for generalist robots, 2024. URL <https://arxiv.org/abs/2406.02523>.
- [26] Soroush Nasiriany, Sepehr Nasiriany, Abhiram Maddukuri, and Yuke Zhu. Robocasa365: A large-scale simulation framework for training and benchmarking generalist robots, 2026. URL <https://arxiv.org/abs/2603.04356>.
- [27] NVIDIA, :, Alisson Azzolini, Junjie Bai, Hannah Brandon, Jiaxin Cao, Prithvijit Chattopadhyay, Huayu Chen, Jinju Chu, Yin Cui, Jenna Diamond, Yifan Ding, Liang Feng, Francesco Ferroni, Rama Govindaraju, Jinwei Gu, Siddharth Gururani, Imad El Hanafi, Zekun Hao, Jacob Huffman, Jingyi Jin, Brendan Johnson, Rizwan Khan, George Kurian, Elena Lantz, Nayeon Lee, Zhaoshuo Li, Xuan Li, Maosheng Liao, Tsung-Yi Lin, Yen-Chen Lin, Ming-Yu Liu, Xiangyu Lu, Alice Luo, Andrew Mathau, Yun Ni, Lindsey Pavao, Wei Ping, David W. Romero, Misha Smelyanskiy, Shuran Song, Lyne Tchampi, Andrew Z. Wang, Boxin Wang, Haoxiang Wang, Fangyin Wei, Jiashu Xu, Yao Xu, Dinghao Yang, Xiaodong Yang, Zhuolin Yang, Jingxu Zhang, Xiaohui Zeng, and Zhe Zhang. Cosmos-reason1: From physical common sense to embodied reasoning, 2025. URL <https://arxiv.org/abs/2503.15558>.
- [28] NVIDIA, :, Johan Bjorck, Fernando Castañeda, Nikita Cherniadev, Xingye Da, Runyu Ding, Linxi "Jim" Fan, Yu Fang, Dieter Fox, Fengyuan Hu, Spencer Huang, Joel Jang, Zhenyu Jiang, Jan Kautz, Kaushil Kundalia, Lawrence Lao, Zhiqi Li, Zongyu Lin, Kevin Lin, Guilin Liu, Edith Llontop, Loic Magne, Ajay Mandlekar, Avnish Narayan, Soroush Nasiriany, Scott Reed, You Liang Tan, Guanzhi Wang, Zu Wang, Jing Wang, Qi Wang, Jiannan Xiang, Yuqi Xie, Yinzhen Xu, Zhenjia Xu, Seonghyeon Ye, Zhiding Yu, Ao Zhang, Hao Zhang, Yizhou Zhao, Ruijie Zheng, and Yuke Zhu. Gr00t n1: An open foundation model for generalist humanoid robots, 2025. URL <https://arxiv.org/abs/2503.14734>.
- [29] NVIDIA, :, Arslan Ali, Junjie Bai, Maciej Bala, Yogesh Balaji, Aaron Blakeman, Tiffany Cai, Jiaxin Cao, Tianshi Cao, Elizabeth Cha, Yu-Wei Chao, Prithvijit Chattopadhyay, Mike Chen, Yongxin Chen, Yu Chen, Shuai Cheng, Yin Cui, Jenna Diamond, Yifan Ding, Jiaojiao Fan, Linxi Fan, Liang Feng, Francesco Ferroni, Sanja Fidler, Xiao Fu, Ruiyuan Gao, Yunhao Ge, Jinwei Gu, Aryaman Gupta, Siddharth Gururani, Imad El Hanafi, Ali Hassani, Zekun Hao, Jacob Huffman, Joel Jang, Pooya Jannaty, Jan Kautz, Grace Lam, Xuan Li, Zhaoshuo Li, Maosheng Liao, Chen-Hsuan Lin, Tsung-Yi Lin, Yen-Chen Lin, Huan Ling, Ming-Yu Liu, Xian Liu, Yifan Lu, Alice Luo, Qianli Ma, Hanzi Mao, Kaichun Mo, Seungjun Nah, Yashraj Narang, Abhijeet Panaskar, Lindsey Pavao, Trung Pham, Morteza Ramezani, Fitsum Reda, Scott Reed, Xuanchi Ren, Haonan Shao, Yue Shen, Stella Shi, Shuran Song, Bartosz Stefanik, Shangkun Sun, Shitao Tang, Sameena Tasmeen, Lyne Tchampi, Wei-Cheng Tseng, Jibin Varghese, Andrew Z. Wang, Hao Wang, Haoxiang Wang, Heng Wang, Ting-Chun Wang, Fangyin Wei, Jiashu Xu, Dinghao Yang, Xiaodong Yang, Haotian Ye, Seonghyeon Ye, Xiaohui Zeng, Jing Zhang, Qinsheng Zhang, Kaiwen Zheng, Andrew Zhu, and Yuke Zhu. World simulation with video foundation models for physical ai, 2026. URL <https://arxiv.org/abs/2511.00062>.
- [30] Ryan Punamiya, Simar Kareer, Zeyi Liu, Josh Citron, Ri-Zhao Qiu, Xiongyi Cai, Alexey Gavryushin, Jiaqi Chen, Davide Liconti, Lawrence Y. Zhu, Patcharapong Aphiwetsa, Baoyu Li, Aniketh Cheluva, Pranav Kuppili, Yangcen Liu, Dhruv Patel, Aidan Gao, Hye-Young Chung, Ryan Co, Renee Zbizika, Jeff Liu, Xiaomeng Xu, Haoyu Xiong, Geng Chen, Sebastiano Olani, Chenyu Yang, Xi Wang, James Fort, Richard Newcombe, Josh Gao, Jason Chong, Garrett Matsuda, Aseem Doriwala, Marc Pollefeys, Robert Katschmann, Xiaolong Wang, Shuran Song, Judy Hoffman, and Danfei Xu. Egoverse: An egocentric human dataset for robot learning from around the world, 2026. URL <https://arxiv.org/abs/2604.07607>.
- [31] Alec Radford, Jong Wook Kim, Chris Hallacy, Aditya Ramesh, Gabriel Goh, Sandhini Agarwal, Girish Sastry, Amanda Askell, Pamela Mishkin, Jack Clark, Gretchen Krueger, and Ilya Sutskever. Learning transferable visual models from natural language supervision, 2021. URL <https://arxiv.org/abs/2103.00020>.
- [32] Mohit Shridhar, Lucas Manuelli, and Dieter Fox. Cliport: What and where pathways for robotic manipulation, 2021. URL <https://arxiv.org/abs/2109.12098>.
- [33] Ishika Singh, Valts Blukis, Arsalan Mousavian, Ankit Goyal, Danfei Xu, Jonathan Tremblay, Dieter Fox, Jesse Thomason, and Animesh Garg. Progprompt: Generating situated robot task plans using large language models, 2022. URL <https://arxiv.org/abs/2209.11302>.

- [34] Qwen Team. Qwen3.5-omni technical report, 2026. URL <https://arxiv.org/abs/2604.15804>.
- [35] Homer Walke, Kevin Black, Abraham Lee, Moo Jin Kim, Max Du, Chongyi Zheng, Tony Zhao, Philippe Hansen-Estruch, Quan Vuong, Andre He, Vivek Myers, Kuan Fang, Chelsea Finn, and Sergey Levine. Bridgedata v2: A dataset for robot learning at scale. In *Conference on Robot Learning (CoRL)*, 2023.
- [36] Jason Wei, Xuezhi Wang, Dale Schuurmans, Maarten Bosma, Brian Ichter, Fei Xia, Ed Chi, Quoc Le, and Denny Zhou. Chain-of-thought prompting elicits reasoning in large language models, 2023. URL <https://arxiv.org/abs/2201.11903>.
- [37] Hongtao Wu, Ya Jing, Chilam Cheang, Guangzeng Chen, Jiafeng Xu, Xinghang Li, Minghuan Liu, Hang Li, and Tao Kong. Unleashing large-scale video generative pre-training for visual robot manipulation, 2023. URL <https://arxiv.org/abs/2312.13139>.
- [38] Seonghyeon Ye, Yunhao Ge, Kaiyuan Zheng, Shenyuan Gao, Sihyun Yu, George Kurian, Suneel Indupuru, You Liang Tan, Chuning Zhu, Jiannan Xiang, Ayaan Malik, Kyungmin Lee, William Liang, Nadun Ranawaka, Jiasheng Gu, Yinzhen Xu, Guanzhi Wang, Fengyuan Hu, Avnish Narayan, Johan Bjorck, Jing Wang, Gwanghyun Kim, Dantong Niu, Ruijie Zheng, Yuqi Xie, Jimmy Wu, Qi Wang, Ryan Julian, Danfei Xu, Yilun Du, Yevgen Chebotar, Scott Reed, Jan Kautz, Yuke Zhu, Linxi "Jim" Fan, and Joel Jang. World action models are zero-shot policies, 2026. URL <https://arxiv.org/abs/2602.15922>.
- [39] Tianhe Yu, Ted Xiao, Austin Stone, Jonathan Tompson, Anthony Brohan, Su Wang, Jaspiar Singh, Clayton Tan, Dee M, Jodilyn Peralta, Brian Ichter, Karol Hausman, and Fei Xia. Scaling robot learning with semantically imagined experience, 2023. URL <https://arxiv.org/abs/2302.11550>.
- [40] Michał Zawalski, William Chen, Karl Pertsch, Oier Mees, Chelsea Finn, and Sergey Levine. Robotic control via embodied chain-of-thought reasoning, 2025. URL <https://arxiv.org/abs/2407.08693>.
- [41] Brianna Zitkovich, Tianhe Yu, Sichun Xu, Peng Xu, Ted Xiao, Fei Xia, Jialin Wu, Paul Wohlhart, Stefan Welker, Ayzaan Wahid, Quan Vuong, Vincent Vanhoucke, Huong Tran, Radu Soricut, Anikait Singh, Jaspiar Singh, Pierre Sermanet, Pannag R. Sanketi, Grecia Salazar, Michael S. Ryoo, Krista Reymann, Kanishka Rao, Karl Pertsch, Igor Mordatch, Henryk Michalewski, Yao Lu, Sergey Levine, Lisa Lee, Tsang-Wei Edward Lee, Isabel Leal, Yuheng Kuang, Dmitry Kalashnikov, Ryan Julian, Nikhil J. Joshi, Alex Irpan, Brian Ichter, Jasmine Hsu, Alexander Herzog, Karol Hausman, Keerthana Gopalakrishnan, Chuyuan Fu, Pete Florence, Chelsea Finn, Kumar Avinava Dubey, Danny Driess, Tianli Ding, Krzysztof Marcin Choromanski, Xi Chen, Yevgen Chebotar, Justice Carbajal, Noah Brown, Anthony Brohan, Montserrat Gonzalez Arenas, and Kehang Han. Rt-2: Vision-language-action models transfer web knowledge to robotic control. In Jie Tan, Marc Toussaint, and Kourosh Darvish, editors, *Proceedings of The 7th Conference on Robot Learning*, volume 229 of *Proceedings of Machine Learning Research*, pages 2165–2183. PMLR, 06–09 Nov 2023. URL <https://proceedings.mlr.press/v229/zitkovich23a.html>.

**Limitations and future work.** Our annotations are produced by a single frozen VLM and inherit its biases. Three open problems remain. First, automatically selecting the right annotation type per task is unsolved: the instructor closes most but not all of the per-task oracle gap, and on a subset of tasks every fixed aspect underperforms the task-only baseline. Second, our experiments are simulation only (RoboCasa 365 and MolmoSpaces); real-robot evaluation would test whether the language-density lever transfers beyond the visual and dynamics distributions of these benchmarks. Third, the four-aspect schema is fixed and chosen heuristically. Natural next steps include scaling beyond a 1M-clip corpus, mixing annotation channels per segment rather than per dataset, and tighter coupling between the instructor and the action policy—for example, training the two jointly so the instructor optimizes directly for downstream action-policy success rather than imitating the offline reward table.

## A DeMiAn Multi-Aspect Annotation

We use Qwen3-VL-30B-A3B-Instruct to generate all four DeMiAn annotation aspects. Each aspect is produced by a separate VLM call conditioned on the segment video, the existing task description, and a context block containing the original task name, available task descriptions, and (for the reasoning aspect on RoboCasa 365) the ground-truth primitive sequence and neighboring segment labels. Each prompt carries a per-aspect length cap. The robot-manipulation datasets (RoboCasa 365 and MolmoSpaces) share one set of prompts written in agent-centric language; EgoVerse uses a separate set adapted to human-egocentric video. We list both sets in the following sections.

### A.1 Robot-manipulation Prompts (RoboCasa 365 and MolmoSpaces)

RoboCasa 365 and MolmoSpaces share the four agent-centric prompts below. Each is issued as a separate VLM call whose user message bundles the segment video, the task description, and the per-aspect instruction.

#### physical\_motion

Describe the physical movement of the agent. For example, if the agent is moving its arm, describe the movement of the arm. If the agent is moving its hand (or the gripper of a robot arm), describe the movement of the hand or the gripper. If the agent is grasping the object, describe the grasping movement of the gripper or hand. If the agent is moving the object, describe the movement of the object. Focus only on the movements within the given frames. Do not hallucinate or make up the action.

#### scene\_composition

Describe the physical environment shown in the video. List the room type, major fixtures, and visible objects on the surfaces (such as specific food items, appliances, or tools).

#### arm\_pose

Describe the exact physical posture and spatial location of the agent’s arm throughout the trajectory. Focus strictly on the arm’s pose (posture, gripper state, orientation) relative to the environment at the start, middle, and end of the clip, without describing the action itself.

#### reasoning

Reason about the agent’s action and environment in the video clips given the task description. The reasoning should be detailed and specific to the video clips, e.g., why the agent is doing this action, what is the goal of the action, what was the previous action, what was the current action, what should be the next action, is the task completed, etc.

## A.2 Human-Egocentric Video Prompts (EgoVerse)

For EgoVerse we recast the same four aspects in human-egocentric language and tighten every prompt to a two-sentence cap, since EgoVerse segments are short and the annotations are concatenated with longer narrations elsewhere in the corpus.

<code>physical_motion</code>
Describe the physical movements of the person’s hands in this clip. Focus on what each hand is doing: reaching, grasping, lifting, pouring, stirring, placing, etc. Mention the objects being manipulated and the direction of movement. Focus only on the movements within the given frames. Do not hallucinate or make up actions.
<code>scene_composition</code>
Describe the physical environment shown in the images. List the setting, workspace surfaces, and visible objects (such as tools, containers, food items, or appliances). Note their spatial arrangement.
<code>arm_pose</code>
Describe the exact position and posture of the person’s hands at the very first frame. What are they holding, touching, or hovering over? Focus strictly on the hands’ state relative to the objects and workspace, without describing the action.
<code>reasoning</code>
Reason about what the person is doing and why, given the task description and the current action annotation. What is the goal of this action segment? What was likely done before this, and what will likely come next? Is this a preparatory step, the main manipulation, or a cleanup step?

## A.3 Annotation Cost Calculation

We use Qwen3-VL-30B-A3B-Instruct through the annotation pipeline. Each VLM call processes one segment video with a text prompt containing the task description and the requested DeMiAn aspect. The script defaults to `max_tokens=256`; empirically and for the scaling plots we approximate each request as  $X_{in} \approx 8.2K$  input tokens (video plus prompt) and  $X_{out} \approx 150$  generated tokens. With Qwen3-VL-30B-A3B’s MoE routing, we charge only the active parameters,  $P_{active} \approx 3 \times 10^9$ , giving

$$F_{call} \approx 2P_{active}(X_{in} + X_{out}) \approx 2 \cdot 3 \times 10^9 \cdot 8.35 \times 10^3 \approx 5.0 \times 10^{13} \text{ FLOPs.}$$

Thus a one-aspect annotation pass over a 1M-clip MolmoBot corpus costs

$$F_{cap} \approx 10^6 F_{call} \approx 5.0 \times 10^{19} \text{ FLOPs.}$$

Using a representative hosted price of \$0.13 per million input tokens and \$0.52 per million output tokens for Qwen3-VL-30B-A3B, this is approximately

$$10^6 \left( 8200 \cdot \frac{0.13}{10^6} + 150 \cdot \frac{0.52}{10^6} \right) \approx \$1.1K$$

for one DeMiAn aspect, or roughly four times larger for annotating all four aspects.

## B Experiment Details

### B.1 Training Details

**DeMiAn VLA.** We adopt the `openpi` model, where the policy applies bidirectional attention over the full prefix of image and language tokens, and is trained with a flow-matching action objective. When reasoning or dense annotation text is included, it is concatenated to the language prompt and receives no token-level supervision. We keep the same bidirectional attention pattern, but add an

annotation-level language-modeling auxiliary loss with weight  $\lambda_{\text{LM}} = 0.1$ . Let the prefix tokens be  $x = (x^{\text{img}}, x^{\text{task}}, x^{\text{cap}})$ , where  $x^{\text{cap}} = (c_1, \dots, c_N)$  are the annotation tokens. Let  $h_i = f_\theta(x)_i$  be the bidirectional transformer output at annotation position  $i$ , and let  $W$  be the tied LM head. The training objective is

$$\mathcal{L} = \mathcal{L}_{\text{FM}} + \lambda_{\text{LM}} \mathcal{L}_{\text{cap}}, \quad \mathcal{L}_{\text{cap}} = -\frac{1}{\sum_{i=1}^{N-1} m_i} \sum_{i=1}^{N-1} m_i \log p_\theta(c_{i+1} | h_i),$$

where  $p_\theta(\cdot | h_i) = \text{softmax}(Wh_i)$  and  $m_i$  is the annotation-token mask.

Because  $h_i$  can attend bidirectionally to later annotation tokens  $c_{>i}$ ,  $\mathcal{L}_{\text{cap}}$  is not a causal likelihood objective and can be partially solved through attention-based copying. We therefore use it only as an auxiliary representation-grounding regularizer: it encourages annotation-token hidden states to remain decodable through the LM head, rather than allowing the bidirectional encoder to compress the annotation into a coarse global summary that may discard object identity, spatial relations, or sub-step structure needed by the action expert. Annotations are produced by an external instructor at inference time, so the model does not generate annotations during deployment and the absence of a causal mask does not create a train-test mismatch.

We post-train two DeMiAn VLA variants from the same backbone, both for 30K steps at global batch size 256 with `openpi`'s default optimizer and learning-rate schedule. The RoboCasa variant fine-tunes `pi05_base` on the RoboCasa 365 atomic-task split with  $\lambda_{\text{LM}} = 0.1$ . The MolmoBot variant fine-tunes `pi05_droid` on the 20% subset MolmoBot corpus without  $\mathcal{L}_{\text{cap}}$  ( $\lambda_{\text{LM}} = 0$ ). For MolmoBot training, we follow the default training mixture that pairs one primary task family (Pick+Place) with three auxiliary families sampled at relative weights 0.25/0.20/0.15 for Pick, NextTo, and Color, respectively.

We use two MolmoBot training scales: the main annotation ablations in Tables 2 and 7 are run on a 20% subset (223K trajectories), while the scaling experiment in Section 4.4 (Figure 5B) uses the full 1M-clip MolmoBot corpus.

**DeMiAn WAM.** 1) *Architecture.* We adopt a prefix-suffix design in the style of GR00T-N1 [28], adapted to the Cosmos-Predict 2.5 video DiT backbone, with a joint blockwise attention variant inspired by  $\pi_{0.5}$  [5]. Cosmos Reason 1 [27] vision-language encoder jointly tokenizes the current observation frame together with the task description into a unified prefix, which the action head consumes via cross-attention. The action head is a four-layer cross-attention stack that runs in parallel to the DiT: each of its  $K=4$  layers taps a DiT block at an evenly spread depth. Within each layer we apply a single joint attention whose queries come only from the action tokens and whose keys and values are the concatenation of (i) the DiT video features at the tapped depth, (ii) the Reason1 vision-language prefix, and (iii) the action queries themselves. The joint attention is followed by a position-wise FFN with hidden ratio 4, and both sub-layers are modulated by AdaLN derived from a sinusoidal time embedding that encodes the flow-matching timestep. Action queries are content-conditioned by a linear projection of the noisy action chunk, and the final action prediction is produced by a zero-initialized linear map onto the 7-DoF action space.

2) *Training.* We train the action head with rectified-flow matching following  $\pi_0$  [5]. When action labels are available, this loss is combined with the DiT's standard video flow-matching objective so the backbone continues to adapt to the target domain; Reason 1 is kept frozen and used as an online prefix encoder. We train with AdamW (learning rate  $5 \times 10^{-5}$ , weight decay  $10^{-5}$ ), a 3K-step warmup, global batch size 256, and 160K total steps: 80K video-only steps, 50K end-to-end steps on the full dataset, and 30K target-task alignment steps.

## B.2 Evaluation Protocol Details

Table 2 reports RoboCasa results for DeMiAn-VLA, averaged across 5 seeds  $\times$  20 episodes per seed for each task. MolmoSpaces test results use a 9-benchmark held-out suite and aggregate per-benchmark success rates into task-family averages.

Table 6: Evaluation protocol summary across the development and test splits used in the paper. In RoboCasa, the seed determines all stochastic elements of the environment (object placement, kitchen layout selection, randomized scene elements).

Parameter	RoboCasa Dev	RoboCasa Test	MolmoSpaces Dev	MolmoSpaces Test
Tasks / benchmarks	17 atomic	17 atomic	6 benchmarks	9 benchmarks
Episodes / unit	20	100	20 (episodes 0–19)	180 (episodes 20–199)
Seed	123-127	42-46	fixed JSON	fixed JSON
Total trials	340	1,700	120	1,620
Max steps / episode	400	400	607	607
Action chunk horizon	8	8	8	8
Env split	target	target	bench-v2 dev subset	bench-v2 test suite
Camera resolution	256×256	256×256	256×256	256×256

Table 7: Per-benchmark success rate as a function of training-time annotation. Values are fractions in  $[0, 1]$ . Columns are grouped by task family with calculated Avg. columns: Pick averages Std/Hard/OOD, Pick+Place averages Std/Hard, and NextTo averages ID/OOD. *w/ Instructor* denotes the learned instruction-generation condition. *Per-task Best (oracle)* takes the column-wise maximum across the annotation rows and serves as an oracle upper bound.

Annotation type	Pick				Pick+Place				NextTo			Color
	Std	Hard	OOD	Avg.	Std	Hard	OOD	Avg.	ID	OOD	Avg.	
<b>DeMiAn VLA</b>												
Baseline	.61	.34	.18	.38	<b>.82</b>	<b>.45</b>	.22	<b>.64</b>	.25	.07	.16	.41
Physical Motion	.73	<b>.45</b>	.24	.47	.76	.44	.18	.60	.20	<b>.13</b>	.17	.46
Scene Composition	.77	<b>.45</b>	.26	<b>.49</b>	.80	.40	.24	.60	.26	.11	.19	.40
Arm Pose	.70	.37	.18	.42	.76	.44	.26	.60	.18	.09	.14	.45
Reasoning	.79	.38	.26	.48	.78	.41	.24	.60	<b>.33</b>	.12	<b>.23</b>	.39
w/ Instructor	<b>.80</b>	.40	<b>.28</b>	<b>.49</b>	.78	.42	<b>.27</b>	.60	.27	<b>.13</b>	.20	<b>.48</b>
Per-task Best (oracle)	.80	.45	.28	.51	.82	.45	.27	.64	.33	.13	.23	.48
<b>DeMiAn WAM</b>												
Baseline	.40	.11	.06	.19	.25	.13	.02	.19	.06	<b>.08</b>	.07	.14
Physical Motion	.44	<b>.15</b>	.08	.22	.27	.15	.06	.21	.07	.05	.06	.15
Scene Composition	.45	.14	<b>.09</b>	.23	.26	.13	.08	.20	.09	.04	.07	.13
Arm Pose	.38	.12	.06	.19	.22	.12	.09	.17	.06	.03	.05	.15
Reasoning	.43	.13	<b>.09</b>	.22	.24	.14	.08	.19	<b>.11</b>	.04	<b>.08</b>	.13
w/ Instructor	<b>.49</b>	.13	<b>.09</b>	<b>.24</b>	<b>.30</b>	<b>.16</b>	<b>.10</b>	<b>.23</b>	.09	.04	.07	<b>.16</b>
Per-task Best (oracle)	.45	.15	.09	.23	.27	.15	.09	.21	.11	.08	.10	.15

## C Extended Results and Analysis

### C.1 Per-Task and Per-Family Annotation Analysis

This section expands on the aggregate RQ1 result of Section 4.1 (Table 2) by walking through which annotation aspect wins on which task and how the pattern differs on MolmoSpaces.

**Per-aspect strengths on RoboCasa.** RoboCasa shows structured heterogeneity rather than a single best annotation type. `physical_motion` tends to help contact-changing manipulation, `scene_composition` helps tasks that require choosing among similar receptacles or surfaces, and `arm_pose` is useful mainly when the task is dominated by body configuration. By contrast, `reasoning` has no unique per-task wins under any fixed aspect, suggesting that subgoal-style annotations alone are often dominated by either motion structure or the learned instructor. The task-only baseline remains strongest on several saturated or annotation-sensitive tasks, so dense annotations are not uniformly beneficial. The same pattern carries over to DeMiAn WAM at lower absolute SR, while *w/ Instructor* converts these complementary strengths into a single policy and uniquely wins tasks that no fixed aspect dominates.

**Per-family patterns on MolmoSpaces.** For DeMiAn VLA, dense annotations clearly help on *Pick*—every fixed aspect lifts the family average over the baseline, with Scene Composition and the learned instructor tied at the top. *Pick+Place* is the one family where the task-only baseline holds its ground on average; individual dense aspects carry pockets of strength on the OOD split, but none beat the baseline overall. *NextTo* flips the winner to Reasoning, whose subgoal-style framing fits the spatial-relation language this family demands; *Color*, in turn, is uniquely won by the instructor. The DeMiAn WAM picture is cleaner: the instructor leads on three of the four families (Pick, Pick+Place, Color), and only *NextTo* again favors Reasoning.

Across both backbones, the takeaway is the same—no fixed aspect is universally best, and the per-family heterogeneity is large enough that selecting the aspect at deployment carries real signal.

## C.2 Instructor Training Details

Table 8: **Results with the Instructor on the RoboCasa Dev set.** All variants share the same action policy checkpoint; only the instruction at inference differs. The *Fixed-aspect GT injection* rows (averaged across the 17 RoboCasa atomic tasks) double as an aggregate view of the reward table  $w(\tau, k)$  used to train the instructor.

Instruction at inference	SR	$\Delta$ vs baseline
Baseline (no annotation)	44.3%	—
<i>Fixed-aspect GT injection (inference-time analogue of Table 2)</i>		
GT physical_motion	46.1%	+1.8
GT scene_composition	48.4%	+4.1
GT arm_pose	47.4%	+3.1
GT reasoning	50.1%	+5.8
Random per-episode aspect	46.6%	+2.3
<i>DeMiAn Instructor variants (async, ours)</i>		
<b>SFT Instructor</b>	<b>50.4%</b>	<b>+6.1</b>
Oracle (per-task-best annotation)	52.4%	+8.1

**Reward table.** The reward table  $w(\tau, k)$  records the action policy’s dev-set SR on each (task  $\tau$ , aspect  $k$ ) pair. We construct it by running the action policy with each of the four GT fixed-aspect annotations across all 17 RoboCasa atomic tasks and recording the resulting SRs. The aspect-wise aggregate of this table is visible in the *Fixed-aspect GT injection* rows of Table 8 (averaged across the 17 tasks); the actual training-time table is per-task and resolves the heterogeneity that this aggregate hides. Tasks where every aspect underperforms the no-annotation baseline are assigned an empty target, teaching the instructor to abstain.

**Training procedure.** We fine-tune Qwen3.5-2B with supervised fine-tuning (SFT). For each training example, we sample a target aspect per task from a softmax over  $w(\tau, \cdot)$  (temperature  $T=2$ , top-3 truncation), and use the pipeline-generated annotation for that (task, aspect) pair as the SFT target—this is the *reward-weighted target sampling* setup described in Section 3. The training set contains 3.2K examples. Training uses  $4 \times$  GB200 GPUs with effective batch size 256, AdamW with cosine schedule.

**Ablations.** We also tested Top-1 SFT (target = the single highest-reward aspect per task) and two DPO variants seeded from SFT (cross-aspect preference pairs ordered by  $w(\tau, k)$ ); none outperformed the default at equivalent training budgets, and length-confounded preference pairs caused DPO to drift toward over-long outputs that hurt the action policy. We therefore use SFT with reward-weighted target sampling as the default recipe.